

Emergent Novel Metallic State in a Disordered 2D Mott Insulator

Elias Lahoud¹, O. Nganba Meetei², K.B. Chaska¹, A. Kanigel¹, Nandini Trivedi²

¹*Physics Department, Technion-Israel Institute of Technology, Haifa 32000, Israel*

²*Department of Physics, The Ohio State University, Columbus, Ohio 43210, USA*

It is well established that for non-interacting electrons, increasing disorder drives a metal into a gapless localized Anderson insulator[1]. While in three dimensions a threshold in disorder must be crossed for the transition, in two dimensions and lower, the smallest amount of disorder destabilizes the metal. The nature of the metal-insulator transition in an interacting system remains unresolved [2–8]. Here we explore the effect of disorder on a strongly correlated Mott insulator without changing the carrier concentration. Angle resolved photoemission spectroscopy (ARPES) measurements on copper intercalated single crystals of the layered dichalcogenide 1T-TaS₂ reveal the presence of new delocalized states within the Mott gap. This is the first experimental realization of a novel disorder-induced metal that was theoretically predicted [9] to exist between the Mott insulator and Anderson insulator.

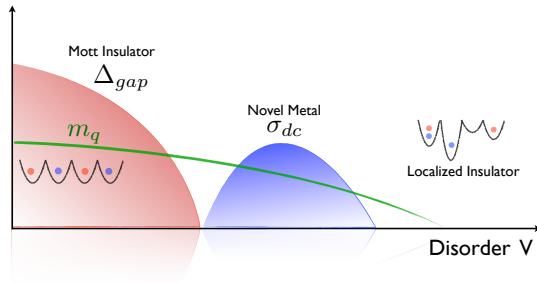


FIG. 1: Schematic figure showing the effect of disordering a Mott insulator (without adding carriers). V is the disorder scale relative to the bandwidth. The charge gap Δ_{gap} in the Mott insulator vanishes at the quantum phase transition to a metal. The novel metal has a finite dc conductivity σ_{dc} and other unusual spectral properties elucidated by ARPES experiments reported here. At higher disorder we expect a second quantum phase transition from the metal to a gapless localized insulator. If the Mott insulator has magnetic order, characterized by the order parameter m_q , it need not be tied to the metal insulator transitions.

The transition-metal dichalcogenide 1T-TaS₂ is a quasi-2D system with strong electron-electron and electron-phonon coupling with a very rich phase diagram. Upon decreasing the temperature, it undergoes several CDW phase transitions: from a high temperature metal-

lic phase to an incommensurate CDW (ICCDW), to a nearly commensurate CDW (NCDW), and finally to a commensurate CDW (CCDW). It even becomes superconducting when subjected to external pressure or chemical disorder [10, 11].

Despite the seemingly complicated electronic properties, 1T-TaS₂ has a simple crystal structure composed of weakly coupled layers, each layer containing a single sheet of tantalum atoms, sandwiched in between two sheets of sulfur atoms. The Ta atoms within each layer form a 2D hexagonal lattice. The basic CDW instability is formed within the tantalum layers by the arrangement of 13 Ta atoms into a “star-of-David” shaped cluster, where 12 Ta atoms move slightly inward towards the 13th central Ta atom (Fig. 2(a)). As temperature is lowered, the size of the CDW domains becomes larger until all the domains interlock into a single coherent CDW modulation extending throughout the layer in the CCDW phase below T_{CCDW} =180K. The new “star-of-David” unit cells form a hexagonal lattice and the corresponding reduced Brillouin zone is depicted by the small green hexagon in Fig. 2(b).

The transition into the CCDW phase is accompanied by a metal-insulator (MI) transition into a Mott phase [1, 2]. The insulating behavior can be clearly seen from resistivity measurements shown in Fig. 2(g). It has been shown [3] that out of the 13 Ta 5d electrons within the “star-of-david” cluster 12 occupy states below the Fermi energy, while the 13th one occupies a half-filled band crossing the Fermi energy. This system is widely regarded as a realization of a half-filled 2D Hubbard model on a triangular lattice where strong electron-electron interaction opens a Mott gap [2].

In this paper, we show that even in the presence of disorder due to Cu intercalation, the CCDW phase exists below T_{CCDW} and that the low energy physics is well described by a disordered half-filled Hubbard model. We therefore have a candidate system for investigating the effect of disorder on a Mott state.

Fig 2(c-d) show the Transmission Electron Microscopy (TEM) images for disordered 1T-TaS₂ above and below T_{CCDW} . The locking of the “star-of-David” clusters results in the appearance of new points in the diffraction image. These points form a small hexagon (green in the figure) rotated by about 13° relative to the large hexagon which represents the basic trigonal unit cell (red in the figure). The results are identical to that of a clean sample (not shown here).

The transition to the CCDW phase can also be seen

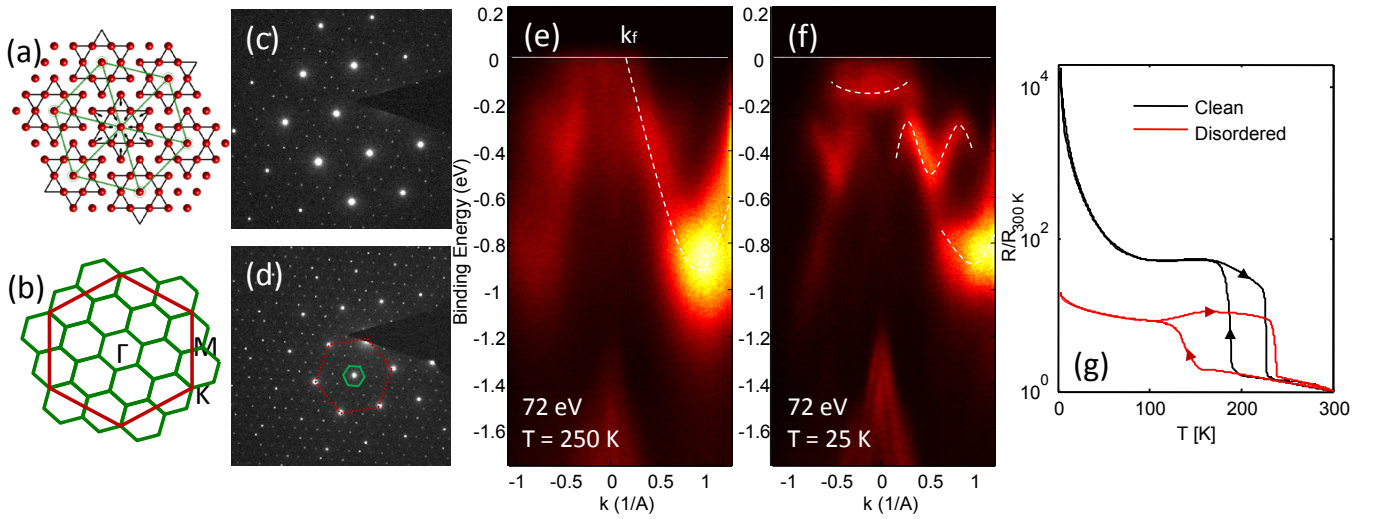


FIG. 2: Mott phase in 1T-TaS₂: (a) visualization of the CCDW phase within a single tantalum sheet and the arrangement of the star-of-David clusters into a triangular lattice. (b) The 2D Brillouin zone of the original triangular Ta sheet (red), and the CCDW phase reconstructed reciprocal unit cells (green). (c-d) TEM diffraction images from a disordered sample in the CCDW phase (T=123K), and the NNCDW phase (T = 223K). (e-f) ARPES data from a disordered sample showing the band dispersion along the Γ -M direction, in the NCCDW and CCDW phases, respectively. The dashed lines are guide to the eye showing the band dispersion. (g) Resistance as a function of temperature on for a clean and a disordered sample, the sample were cooled from 300K down to 2K and back to 300K.

directly using APRES. In Fig 2(e-f) we show ARPES (experimental details are given in the Methods section) spectra taken above and below the transition. Above the transition we observe a parabolic band with a bandwidth of about ≈ 1 eV, originating from the Ta 5d orbital[15], dispersing upwards from M towards the Γ point, and crossing the Fermi energy at 25 % of the $\Gamma - M$ distance (dashed line Fig 2(e)). At 25K this band is split into three sub-bands due to the CCDW reconstruction (Fig 2(f)). The same reconstruction happens in the clean case also (Fig. 3(a)). Notice that the upper most sub-band, laying closest to the Fermi energy, is well separated in energy from the rest and has a bandwidth of about $W \approx 45$ meV. The Coulomb on-site energy U is evaluated to be on the order of 0.1eV [10]. Therefore, the low energy physics can be described by a single band model with the value of $U/W \approx 2.2$ well over the critical value for the Mott transition ($U_C/W \approx 1.3$)[16].

Finally, we see a large hysteresis in the resistivity measurements as a function of temperature as shown in Fig. 2(g). This is characteristic of a first order phase transition into the CCDW phase. Disorder changes somewhat the transition temperature and the hysteresis. Collectively, all the experimental data suggests that the commensurate inter-locking of the “star-of-David” clusters in the CCDW phase is not affected by Cu intercalation.

We next investigate the effect of disorder on the low energy spectral properties. In Fig 3(a-b) we show a comparison of APRES data of a clean and a disordered sample, at the same crystal orientation along the $\Gamma - K$ direction measured with 22 eV photon energy. There is a

significant increase in the spectral intensity in the disordered sample in the $[-0.1 \text{ eV}, 0 \text{ eV}]$ energy range which appears to be centered at the Γ point. Looking at the EDCs at the Γ point in Fig 3(c) one can see the transfer of spectral weight towards lower binding energy in the disordered sample, with a line shape that is slightly skewed towards $E=0$. The symmetrized EDC (Fig3(d)) confirms the presence of a “soft” gap, where the spectral weight at zero energy is about 20 % of the intensity at the peak and the broad peaks are shifted inwards, leaving a smaller Mott gap. The filling up of Mott gap is accompanied by a transition from insulating to metallic behavior in resistivity (Fig. 2(g)). However, it is a very unusual disorder driven metal with no Fermi liquid like spectral peak at $\omega = 0$. In Fig. 3(e) we plot the EDC’s at the Γ point for 13 different clean and disordered crystals. The results are highly reproducible, although the data shown here were measured in different ARPES setups and the crystals are from several different growth batches.

The temperature dependence of the symmetrized EDC at Γ is shown in Fig. 3(f) for a clean and disordered sample. The difference in line shape and in the shape of the gap is most prominent at low temperatures, and the EDCs become increasingly similar as temperature is raised.

To gain better insight into our experimental results, we investigate the effect of disorder on a Mott insulator using a half-filled single band Hubbard model on a triangular

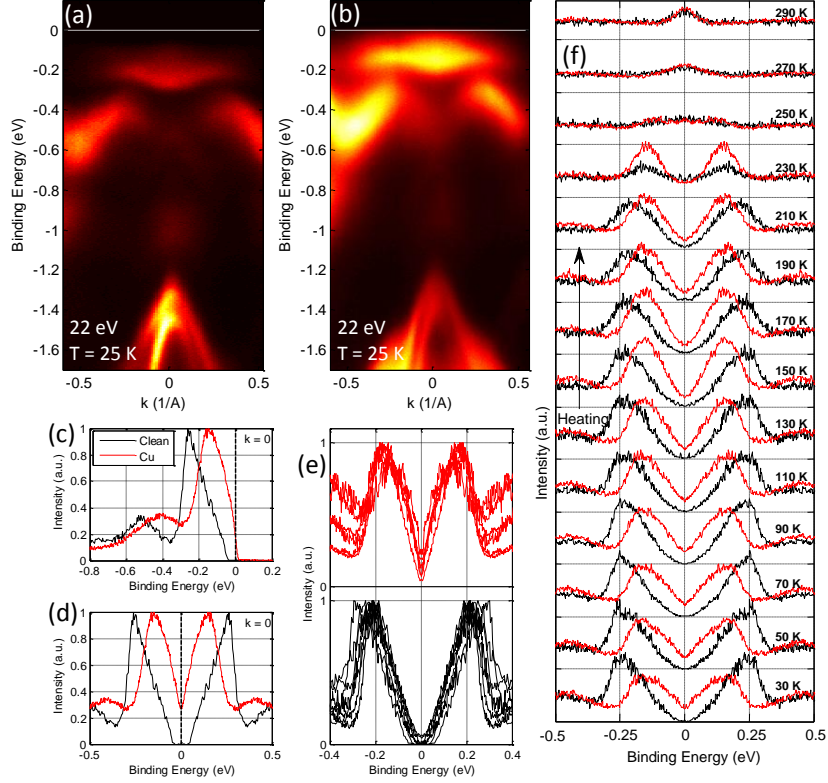


FIG. 3: The electronic structure of a disordered Mott-insulator: (a) ARPES data from a 1T-TaS₂ crystal taken with 22eV photons along the $\Gamma - K$ direction at $T < T_{CCDW}$, reveal a Mott gap in the spectrum as indicated by the lack of intensity within about 80 meV of the Fermi energy. (b) ARPES data from a disordered samples measured under the same conditions; significant amount of spectral weight is now present close to the Fermi energy, inside the energy gap. (c) Comparison of the EDC at the Γ point taken from the scans in (a) and (b). The peak in the disordered 1T-TaS₂ is broadened and shifted towards lower binding energy and there is substantial amount of intensity at zero energy. (d) The same EDCs shown in (c) after symmetrization, clearly reveals the closing of the gap in the disordered sample, the intensity at the Fermi-level is about 20 % of the peak-intensity. (e) Reproducibility of the results: EDCs from 13 different samples (7 clean and 6 disordered) taken in different ARPES systems with different photon energies and polarizations, all reveal the same qualitative behavior. (f) Symmetrized EDCs at the Γ point as function of the temperature. The samples were first cooled to base temperature and measured while warming to room temperature. While at low temperatures the spectral weight at zero energy is much larger in the disordered samples, above the CCDW transition temperature the spectral weight at zero in the clean and disordered sample is the same.

lattice. It describes the CCDW phase of 1T-TaS₂.

$$H = -t \sum_{\langle ij \rangle, \sigma} (c_{i\sigma}^\dagger c_{j\sigma} + h.c.) - t' \sum_{\langle\langle ij \rangle\rangle} (c_{i\sigma}^\dagger c_{j\sigma} + h.c.) + \sum_{i, \sigma} (\epsilon_i - \mu) c_{i\sigma}^\dagger c_{i\sigma} + U \sum_i n_{i\uparrow} n_{i\downarrow} \quad (1)$$

Here t is the nearest-neighbor hopping between unit cells, t' the next nearest hopping, μ , the chemical potential and U , the on-site interaction strength. $c_{i\sigma}^\dagger$ ($c_{i\sigma}$) creates (annihilates) an electron of spin σ at site i , and $n_{i\sigma} = c_{i\sigma}^\dagger c_{i\sigma}$ is the number operator for spin σ at site i . The onsite disorder potential ϵ_i , with a flat distribution in the range $[-V/2, V/2]$, captures the effect of lattice distortions due to Cu intercalation. In our analysis, addition of Cu does not change the filling. We solve

Eq. 1 within inhomogeneous mean-field theory where independent mean-field parameters at each site are determined self-consistently (details in Supplementary Material). For a given disorder realization, we obtain the single particle eigenstates $\{|\Psi_\alpha\rangle\}$ and eigenvalues $\{\epsilon_\alpha\}$ which can be used to calculate the single particle Green's function

$$G(\mathbf{r}_1, \mathbf{r}_2, \omega) = \sum_\alpha \frac{\langle \mathbf{r}_1 | \psi_\alpha \rangle \langle \psi_\alpha | \mathbf{r}_2 \rangle}{\omega + i\eta - \epsilon_\alpha} \quad (2)$$

Upon disorder averaging, and then Fourier transforming, we finally get the spectral function $A(\mathbf{k}, \omega) = -(1/\pi) \text{Im} G(\mathbf{k}, \omega)$ which we compare with experimental results below.

EDC of spectral function: At half-filling in the clean limit with $t' = 0$, mean field solutions gives an insulator

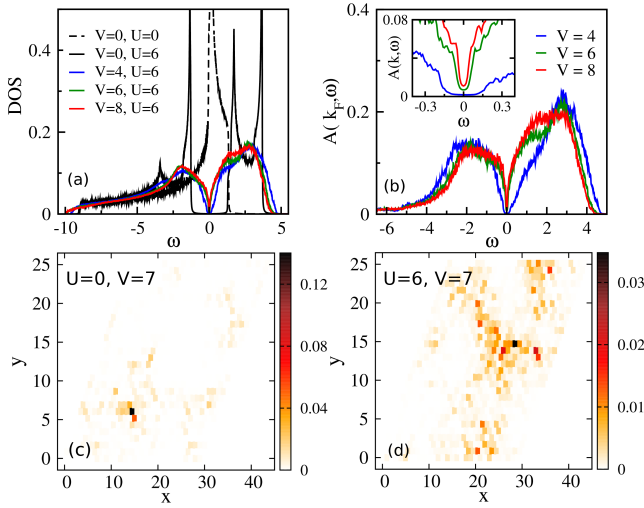


FIG. 4: (a) Theoretical density of states for different disorder strengths V and fixed interaction $U = 6t$. (b) EDC of spectral function at $k = k_F$ for $U = 6t$ and different values of disorder strength V . For weak disorder ($V < U$), there is a well formed gap which closes as disorder is increased ($V \gtrsim U$). Inset: Spectral weight at $\omega = 0$ as a function of disorder strength. For $V \gtrsim U$ there is spectral weight at $\omega = 0$. We used 18×18 size lattices for the calculations averaged over 100 disorder realizations. (c) and (d) shows probability density of $\omega = 0$ eigenstate as a function of position for $U = 0$ and $U = 6t$ respectively with $V = 7t$. The eigenstate is extended over the entire lattice for $U = 6t$. The scale is cut off at the maximum value of $|\Psi(i)|^2$ in each case.

for $U > U_c \simeq 5.27t$ [17] along with magnetic ordering of the spins on the triangular lattice in a commensurate 120° pattern. For the rest of the calculation, we choose $U = 6t$ in order to remain in the insulating phase. Inclusion of $t' = 0.3t$ does not affect the magnetic ground state, but is important for producing a realistic band structure for comparison with experiments. Small change in filling ($\delta n < 2\%$) also does not change the mean-field solution.

Previous studies have observed a suppression in the total density of states around $\omega = 0$ persisting up to large values of disorder [18–20]. Here we obtain information about the spectral function in Fig. 4(b). The EDC at the Fermi momentum for different amounts of disorder can be compared directly with the experimental results shown in Fig. 3(c-d). Our theoretical results agree qualitatively with our experimental results on several aspects. First of all, with increasing disorder the Mott gap closes and finite spectral weight develops at $\omega = 0$ (see inset of Fig. 4(b)). Second, the shape of the gap changes from a hard ‘U’ shaped gap in the clean limit to a ‘V’ shaped soft gap in the disordered case. Finally, the position of the broad peaks corresponding to the upper and lower Hubbard bands move closer to the chemical potential with increasing disorder in agreement with experimental

data. It should be pointed out that the spectral function from theory is asymmetric around $\omega = 0$ and is due to the underlying asymmetry of the density of states (DOS) shown in Fig. 4(a). The experimental data has been symmetrized around $\omega = 0$ to remove the effect of the Fermi factor for small energies ($\omega \ll \Delta$ where Δ is the gap between the broad peaks). Comparison between theory and experiment should be made only for small ω .

In our calculation, the additional low frequency weight upon disordering the system arises primarily from k -states close to the underlying Fermi surface of the tight-binding model. In the experimental data in Fig. 3(b), on the other hand, the additional weight appears from states close to the Γ point. The discrepancy could be due to experimental resolution or possibly due to magnetic ordering and the resultant zone folding that can also push the weight close to the Γ point.

Mid-gap states: The crucial question to ask is about the nature of states filling up the Mott gap when disorder is introduced. The scaling theory of Anderson localization for non interacting electrons predicts that these states should be localized, however, the interplay of strong interaction and disorder can lead to a novel metallic phase [9]. We confirm here that the eigenstates close to the chemical potential are indeed extended on a triangular lattice for $V \approx U$ (See Fig. 4(c-d)). This is further confirmed by the observation of a drastic drop in resistivity of Cu intercalated 1T-TaS₂ in the CCDW phase in comparison to the clean samples (Fig. 2(g)), thereby providing evidence for the emergence of this novel metal.

In conclusion, the remarkable “star-of-David” reconstruction and the strong correlations on the Ta 5d orbitals conspire to make 1T-TaS₂ a realization of a single orbital Mott insulator on a triangular lattice. We have found that 1T-Cu_xTaS₂ with small values of x (less than 1%) does not destroy the underlying CDW state showing crucially that Cu intercalation disorders the system but does not add carriers. Using ARPES we have shown that disorder destroys the Mott gap and introduces electronic states at zero energy. Based on the comparison between the theoretical results and the ARPES and transport experiments, we conclude that 1T-Cu_xTaS₂ is the first example of a novel metallic phase in a disordered 2D Mott insulator. This conducting state is a non-Fermi liquid metal with a pseudogap in the spectral function. Our investigations open up the possibility of several future explorations of the nature of magnetism, its evolution with disorder and its relation to the metal-insulator transitions.

METHODS

Sample Preparation

Single crystals of 1T-TaS₂ were prepared using the vapor transport method as described in Ref. [22]. For the addition of disorder, we added 10 % Cu into the stoichiometric mix during the crystal growth stage. However, the copper content of the single crystals that emerge from the growth is well below 10 %. In fact, wave dispersive electron spectroscopy places the Cu content of the sample at $0.75\% \pm 0.05\%$. The Cu atoms are expected to reside as intercalation between the TaS₂ layers[21]. These samples, which we shall refer to as disordered 1T-TaS₂, display a lower NCCDW-CCDW transition temperature of around 150 K upon cooling (Fig. 2(g)), and the negative slope of $R(T)$ is also considerably reduced compared to the clean sample, suggesting enhanced conductivity.

ARPES

We have performed extensive angle-resolved photoemission spectroscopy (ARPES) measurements, on the PGM-beam line at the Synchrotron Radiation Center with 72 eV and 22 eV photon energy as well as at the ARPES machine at the Technion, using the HeI 22 eV spectral line from discharge lamp as the light source. In both cases data was collected using a scienta R4000 electron analyzer. Samples were cleaved in-situ at a pressure better than 5×10^{-11} torr. Energy and angular resolution were better than 10 meV and 0.3° .

[1] Abrahams, E., Anderson, P. W., Licciardello, D. C. & Ramakrishnan, T. V. Scaling theory of localization: Absence of quantum diffusion in two dimensions. *Phys. Rev. Lett.* **42**, 673 (1979).

[2] Lee, P. A. & Ramakrishnan, T. V. Disordered electronic systems. *Rev. Mod. Phys.* **57**, 287 (1985).

[3] Abrahams, E., Kravchenko, S. V. & Sarachik, M. P. Metallic behavior and related phenomena in two dimensions. *Rev. Mod. Phys.* **73**, 251–266 (2001).

[4] Kravchenko, S. V. & Sarachik, M. P. Metalinsulator transition in two-dimensional electron systems. *Rep. Prog. Phys.* **67**, 1–44 (2004).

[5] Kravchenko, S. V., Kravchenko, G. V., Furneaux, J. E., Pudalov, V. M. & D'Iorio, M. Possible metal-insulator transition at $B = 0$ in two dimensions. *Phys. Rev. B* **50**, 8039–8042 (1994).

[6] Punnoose, A. & Finkel'stein, A. M. Metal-Insulator transition in disordered Two-Dimensional electron systems. *Science* **310**, 289–291 (2005).

[7] Vojta, T., Epperlein, F. & Schreiber, M. Do interactions increase or reduce the conductance of disordered electrons? it depends! *Phys. Rev. Lett.* **81**, 4212–4215 (1998).

[8] Dobrosavljević, V., Trivedi, N. & Valles, J. *Conductor-Insulator Quantum Phase Transitions* (Oxford University Press, 2012).

[9] Heidarian, D. & Trivedi, N. Inhomogeneous metallic phase in a disordered mott insulator in two dimensions. *Phys. Rev. Lett.* **93**, 126401 (2004).

[10] Sipos, B. *et al.* From mott state to superconductivity in 1T-TaS₂. *Nat. Mater.* **7**, 960 (2008).

[11] Xu, P. *et al.* Superconducting phase in the layered dichalcogenide 1T-TaS₂ upon inhibition of the metal-insulator transition. *Phys. Rev. B* **81**, 172503 (2010).

[12] Wilson, J., Di Salvo, F. & Mahajan, S. Charge-density waves and superlattices in the metallic layered transition metal dichalcogenides. *Adv. Phys.* **24**, 117–201 (1975).

[13] Fazekas, P. & Tosatti, E. Charge carrier localization in pure and doped 1T-TaS₂. *Physica B&C* **99**, 183–187 (1980).

[14] Whangbo, M. H. & Canadell, E. Analogies between the concepts of molecular chemistry and solid-state physics concerning structural instabilities. electronic origin of the structural modulations in layered transition metal dichalcogenides. *J. Am. Chem. Soc.* **114**, 9587–9600 (1992).

[15] Rossnagel, K. & Smith, N. V. Spin-orbit coupling in the band structure of reconstructed 1T-TaS₂. *Phys. Rev. B* **73**, 073106 (2006).

[16] Aryanpour, K., Pickett, W. E. & Scalettar, R. T. Dynamical mean-field study of the mott transition in the half-filled hubbard model on a triangular lattice. *Phys. Rev. B* **74**, 085117 (2006).

[17] Krishnamurthy, H. R., Jayaprakash, C., Sarker, S. & Wenzel, W. Mott-hubbard metal-insulator transition in nonbipartite lattices. *Phys. Rev. Lett.* **64**, 950–953 (1990).

[18] Chiesa, S., Chakraborty, P. B., Pickett, W. E. & Scalettar, R. T. Disorder-induced stabilization of the pseudogap in strongly correlated systems. *Phys. Rev. Lett.* **101**, 086401 (2008).

[19] Shinaoka, H. & Imada, M. Soft hubbard gaps in disordered itinerant models with short-range interaction. *Phys. Rev. Lett.* **102**, 016404 (2009).

[20] Wortis, R. & Atkinson, W. A. Physical mechanism for a kinetic energy driven zero-bias anomaly in the anderson-hubbard model. *Phys. Rev. B* **82**, 073107 (2010).

[21] Morosan, E. *et al.* Superconductivity in Cu_xTiSe₂. *Nat. Phys.* **2**, 544 (2006).

[22] Di Salvo F.J., Maines R.G. and Waszczak J.V. and Schwall R.E., ,Preparation and properties of 1T-TaSe₂, *Soild State Comm.* **14**, 497 (1974).

SUPPLEMENTARY MATERIAL

Disorder effects in the NCCDW

We verify that the new states reported in the paper are linked to the underlying Mott state by searching for any sign of increased spectral weight near the Fermi level in the normal metal phase that emerges from the non-commensurate charge density wave (NCCDW) phase. In Fig. 1 we compare the EDCs at the Γ point and at k_F of clean and a disordered sample. The samples were cleaved and measured at 300 K and the data normalized by the

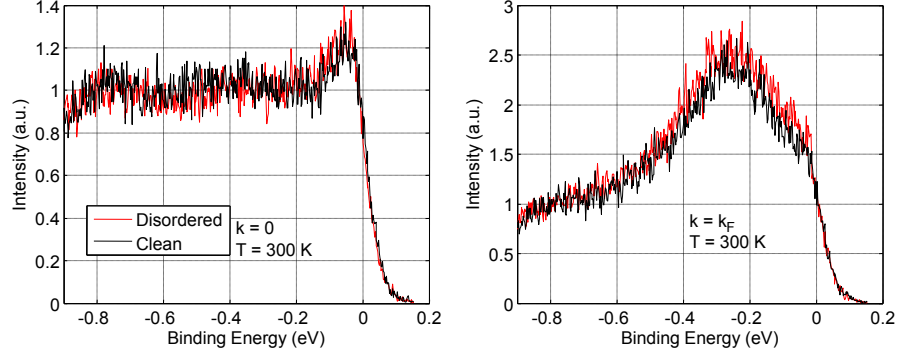


FIG. 1: EDCs of a clean and disordered sample taken with 22 eV photon energy at room temperature at Γ in (a) and at k_F in (b).

intensity at -0.8 eV. The EDC's are identical and this remains the case throughout the Brillouin zone. We find no trace of the new states when the disordered sample is not in the Mott state. In addition, we measured very carefully the position of the top of the Sulfur band with respect to the Fermi-level. The top of Sulfur band at about 1.2 eV below the Fermi-level is relatively sharp and can be used to measure the chemical-potential. We found no measurable effect of Cu intercalation on the chemical-potential. We conclude that if indeed the Cu intercalation induces new states, these states cannot account for the additional spectral intensity within the Mott gap in the commensurate CDW (CCDW) phase.

TEM

Transmission Electron Microscopy (TEM) probes the periodic structure in the material and is ideal for detecting the presence of the electronic CDW modulation in the sample, and identifying the different phases of TaS₂. The CCDW-NCCDW transition can be seen in the clean sample in Fig. 2 (top panels), above the transition the brightest spots correspond to the diffraction from the undistorted hexagonal Ta sheets, and the larger dim hexagons are associated with the formation of the "star-of-david" unit structure. Below the transition the stars interlock and tile the entire Ta sheet, yielding the new diffraction peaks below the transition. We observed exactly the same behavior in the disordered samples, as shown Fig. 2 (bottom panels). The addition of Cu did not suppress the CCDW phase. The electron diffraction images were acquired using a FEI Tecnai T20 Transmission Electron Microscope (TEM), using a Gatan double-tilt cryo-stage (liquid N₂). The samples were cooled down to 100K and then warmed up back to room temperature.

Inhomogeneous mean field theory

The commensurate CDW (CCDW) phase of 1T-TaS₂ is widely regarded as a realization of half-filled 2D Hubbard model on a triangular lattice [1–3]. Of the 13 Ta 5d electrons in the "star-of-David" unit cell 12 occupy states below the Fermi energy, while the 13th electron occupies a half-filled band crossing the Fermi energy. In the case of Cu intercalated samples, we need to include the effect of disorder also, which we model as on-site potential disorder. The model Hamiltonian is (Eq. (1) in main text)

$$H = -t \sum_{\langle ij \rangle, \sigma} (c_{i\sigma}^\dagger c_{j\sigma} + h.c.) - t' \sum_{\langle\langle ij \rangle\rangle} (c_{i\sigma}^\dagger c_{j\sigma} + h.c.) + \sum_{i, \sigma} (\epsilon_i - \mu) c_{i\sigma}^\dagger c_{i\sigma} + U \sum_i n_{i\uparrow} n_{i\downarrow} \quad (1)$$

Here t is the nearest-neighbor hopping between unit cells, t' the next nearest hopping, μ , the chemical potential and U , the on-site interaction strength. $c_{i\sigma}^\dagger (c_{i\sigma})$ creates(annihilates) an electron of spin σ at site i , and $n_{i\sigma} = c_{i\sigma}^\dagger c_{i\sigma}$ is the number operator for spin σ at site i . The onsite disorder potential ϵ_i , with a flat distribution in the range $[-V/2, V/2]$, captures the effect of lattice distortions due to Cu intercalation. In our analysis, addition of Cu does not change the filling.

We solve Eq. 1 within inhomogeneous mean-field theory. The interaction term is approximated as

$$n_{i\uparrow} n_{i\downarrow} \approx n_{i\uparrow} \langle n_{i\downarrow} \rangle + \langle n_{i\uparrow} \rangle n_{i\downarrow} - \langle n_{i\uparrow} \rangle \langle n_{i\downarrow} \rangle - \langle S_i^+ \rangle S_i^- - \langle S_i^- \rangle S_i^+ + \langle S_i^+ \rangle \langle S_i^- \rangle \quad (2)$$

where the operator $\mathbf{S} = \sum_{\sigma, \sigma'} c_{i\sigma}^\dagger \boldsymbol{\tau}_{\sigma, \sigma'} c_{i\sigma'}$ and $\boldsymbol{\tau}$ are the Pauli spin matrices. Due to the presence of disorder, the density and spin fields are site-dependent and the $3N$ parameters $\{\langle n_{i\sigma} \rangle, \langle S_i^+ \rangle = \langle S_i^- \rangle^*\}$, $i = 1, \dots, N$ and $\sigma = \uparrow$ or \downarrow , where N is the total number of sites, are obtained by a self-consistent solution of the coupled inhomogeneous Hartree-Fock equations. Once self-consistency is

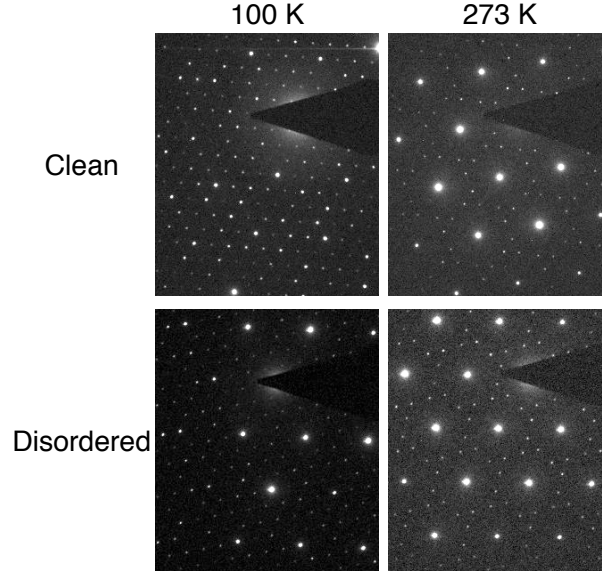


FIG. 2: TEM diffraction images of a clean and disordered samples in the CCDW phase (left panels) and in the NCCDW phase (right panels)

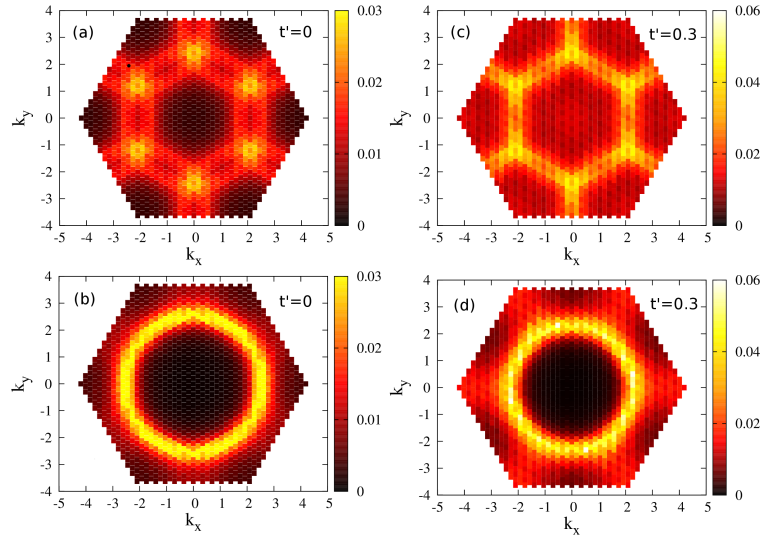


FIG. 3: (a)&(c): Momentum distribution cut (MDC) of disorder averaged spectral function at $\omega = 0$ plotted in the magnetic Brillouin zone (dotted hexagon) for $t' = 0$ and $t' = 0.3t$ respectively. (b)&(d): The same MDC plot as in (a) and (c) but in the non-magnetic Brillouin zone. $V=7t$ and $U=6t$

reached, we obtain the single particle eigenstates and eigenvalues, and use them to calculate the spectral function. For a given disorder realization, the single particle Green's function is given by (Eq. (2) in main text)

$$G(\mathbf{r}_1, \mathbf{r}_2, \omega) = \sum_l \frac{\langle \mathbf{r}_1 | \psi_l \rangle \langle \psi_l | \mathbf{r}_2 \rangle}{\omega + i\eta - \epsilon_l} \quad (3)$$

where $|\psi_l\rangle$ is the mean-field eigenstate with eigenvalue ϵ_l .

Upon disorder averaging, we obtain the translationally invariant Green's function, $G(\mathbf{r}_1, \mathbf{r}_2, \omega) \rightarrow G(\mathbf{r}_1 - \mathbf{r}_2, \omega)$ which can be Fourier transformed to get the Green's function in momentum space, $G(\mathbf{k}, \omega)$. The spectral function can finally be calculated as

$$A(\mathbf{k}, \omega) = -\frac{1}{\pi} \text{Im} G(\mathbf{k}, \omega) \quad (4)$$

Magnetic order: Inhomogeneous mean-field theory

predicts magnetic order with the commensurate 120° pattern even in the presence of disorder. While there is no direct experimental evidence of magnetic order, the APRES data shown in Fig. (3) of main text show significant $\omega = 0$ spectral weight at the Γ -point. We can reproduce the spectral weight at Γ -point from theory only if we include the zone folding effect of the magnetic lattice in k -space. Fig. 3(b) and (d) show the momentum distribution cut (MDC) of the spectral weight at $\omega = 0$ for two different values of t' (next-nearest hopping amplitude) plotted in the non-magnetic Brillouin zone. There is negligible spectral at the Γ -point. In comparison, Fig. 3(a) and (c) which are plotted in the magnetic Brillouin zone (dotted hexagon) show significant spectral weight at the Γ -point. The observed spectral weight at the Γ point suggests enhanced magnetic correlations at the commensurate ordering wave vector. We predict that

experiments performed at lower temperatures should observe long range magnetic order.

-
- [1] Wilson, J., Di Salvo, F. & Mahajan, S. Charge-density waves and superlattices in the metallic layered transition metal dichalcogenides. *Adv. Phys.* **24**, 117–201 (1975).
 - [2] Fazekas, P. & Tosatti, E. Charge carrier localization in pure and doped 1T-TaS₂. *Physica B&C* **99**, 183–187 (1980).
 - [3] Whangbo, M. H. & Canadell, E. Analogies between the concepts of molecular chemistry and solid-state physics concerning structural instabilities. electronic origin of the structural modulations in layered transition metal dichalcogenides. *J. Am. Chem. Soc.* **114**, 9587–9600 (1992).